Journal of
NANOSTRUCTURES

JNS
NANOSTRUCTURES
JNS.kashanu.ac.ir

Ultrasonic Assisted Adsorption of Basic Dyes from Binary Component Systems onto ZnO Nanoparticles Loaded on Activated Carbon Derived from Almond Shell: Optimization by Central Composite Design

A. Asghari *[a], M. Hemati[a], M. Ghaedi [b], M. Rajabi [a], B. Mirtamizdoust[c]

[a]*Department of Chemistry, Semnan University, Semnan 35195-363, Iran*

[b]*Department of Chemistry, Yasouj University, Yasouj 75918-74831, Iran*

[c]*Department of Chemistry, Faculty of Science, University of Qom, Qom 37185-359, Iran*

*Corresponding author:
E-mail address:
aasghari@semnan.ac.ir
Tel: (98) 23 33383193
Fax: (98) 23 33654110

Abstract

In this study, ZnO nanoparticles were loaded on activated carbon prepared from almond shell (ZnO-NP-AC). Then, this novel material applied as an efficient adsorbent for the ultrasonic assisted simultaneous removal of Basic Blue 41(BB41) and Basic Red 46 (BR46) in binary solution. The efficiency of proposed activated carbon was enhanced by acid treatment and subsequent modification by physical mixing with ZnO- NP. The identification by different techniques such as FT-IR, SEM and XRD confirm its porous structure and appearance of various functional groups on AC. In batch process mode, the effect of variables such as adsorbent dosage, initial dyes concentration and sonication time on the removal of dyes were studied by central composite design (CCD) combined with response surface methodology (RSM) and desirability function (DF). The optimum values of input variables were found to be 0.03 g of adsorbent, 19 min of sonication time, 14 mg/L of BR46, 9 mg/L of BB41in pH 6 to high removal percentage (85% and 91% for BR 46, BB41, respectively). Among of the conventional isotherm and Kinetic models, p-factor and second-order models showed reasonable fit to the adsorption equilibrium data, respectively.

1. Introduction

The presence of dyes and pigments in industries wastewaters are hazardous for human and animals health due to their toxic, carcinogenic and even mutagenic effects. They possess adverse effect on the photosynthesis because of the reduction of light penetration to water [1]. According to chemical structure classified to azo, diazo, anthraquinone,
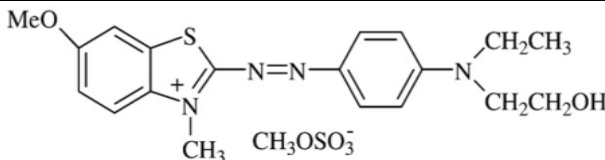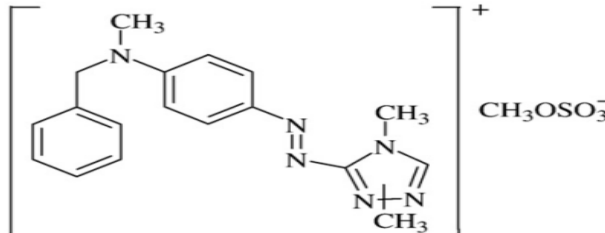
nitro and nitrozo categorys. Also according to their charge and auxochrome divided into cationic and anionic dyes, while among them, azo and cationic dyes can be more toxic because of the production of hazardous aromatic amines under anaerobic conditions. In addition, degradation of cationic dyes is more difficult than anionic dyes. Cationic dyes (basic dyes) widely used in acrylic, nylon, silk and wool dyeing.

There are many pathways to remove dyes from colored effluents such as oxidation, flocculation, coagulation, membrane filtration, photocatalysis, electrochemical techniques and adsorption. Most of the dyes are stable to light, heat and many oxidizing agents [2, 3]. Therefore, Adsorption has been found to be superior to the other techniques for dye wastewater treatment in terms of simplicity of design, ease of operation and ability to use the large variety of cheap, non-toxic materials as

adsorbent possesses high efficiency adsorption capacity [4, 5].

Activated carbon is the effective adsorbent due to its large surface area, high porosity and high adsorption capacity, however; the high cost of activated carbon and incomplete regenerability has been limited its application. Hence; special attention has been given to agricultural wastes such as sawdust, waste tea, rice husk, peels of pineapple, orange, banana and shells of almond, pineapple, walnut and etc. [1, 6, 7]. But the carbon obtained from agricultural wastes has low porosity and surface area. So the surface chemistry of carbon can be modified by various methods, such as, acid treatment, oxidization, ammonization, plasma and microwave treatment [7, 8]. Acid treatment not only removes impurities via oxidization of carbon surface but also improves its porosity. In addition, this method produces OH, COOH and C=O groups on the surface that

Table 1. The properties of basic dyes.

Chemical structure	Commercial name	CAS NO.	λ_{max} (nm)	M_w (g/m
	Basic Blue 41	12270-13-2	607	482
	Basic Red 46	12221-69-1	530	432

enhances its acidic properties [9-11]. Application of nanomaterials in adsorption is useful for solving these problems, so that the presence of reactive groups such as hydroxyl, carbonyl and carboxylic acids enhance the linkage of carbon and

nanomaterial. In fact, nanomaterial can improve dyes removal percentage via increasing the surface area and number of reactive centers [12, 13].

Normal spectrophotometric method cannot perform quantitative analysis of binary and ternary

dye solutions due to highly overlapping spectra. The derivative spectrophotometry technique is good and well known procedure to resolve these limitations. Derivative spectrophotometry can simultaneously analyze multi-component dye mixtures without initial separation or purification [14,15]. Therefore it is more economic and simpler than other techniques such as chromatography, capillary electrophoresis and so on.

Effective parameters on ultrasound assisted adsorption method are sonication time, adsorbent dosage, pH and initial dyes concentration. Univariate and Multivariate methods are helpful approaches for optimization of variables influence. In Univariate method, the response is investigated for each factor while all other factors are held at a constant level. It is more time consuming due to high numbers of experiments, while has low ability for estimation of interaction between factors. Alternatively, multivariate methods such as response surface methodology (RSM), combination of mathematical and statistical techniques, is suggested for designing experiments and building models [16-20].

In this research, CCD combined with RSM was used as the experimental design for ultrasonic assisted adsorption of basic dyes onto ZnO nanoparticles loaded on activated carbon derived from almond shell. The simultaneous analysis of BR46, BB41 in binary solution was performed using derivative spectroscopy following application of ultrasound irradiation that accelerates the dyes removal by increasing mass transfers. Finally; extended Langmuir and Freundlich isotherm models in addition to kinetic models such as pseudo first order, pseudo second Order, Elovich and intraparticle diffusion equations were applied to investigate the equilibrium and rate of adsorption process, respectively.

2. Experimental procedure
2.1. Materials

Almond sells was obtained from the central northern portion of Iran (Semnan). Basic Blue 41 (BB41) and Basic Red 46 (BR46) were purchased from Daystar Firm with commercial names Astrazon Blue FGGL and Astrazone Red FBL. The chemical structure and properties of the dyes are shown in Table 1. All other chemicals including HNO_3, HCl, NaOH with the highest purity available were purchased from Merck (Germany).

2.2. Instruments

A Shimadsu, UV-Vis 1650 PC spectrophotometer was used to measure the absorbance spectra of BB41 and BR46 in the range of 200–700 nm by a quartz cell with an optical path of 1 cm. A BEL PHS-3BW pH-meter with a combined glass-Ag/AgCl electrode was used for adjustment of test solution pH. An ultrasonic bath at50/60kHz of frequency (SW3, Switzerland) was used for the ultrasound-assisted adsorption method. FT-IR spectra were recorded with a Shimadzu 8400 double beam spectrophotometer in the range of $4000 - 400 \ cm^{-1}$ with KBr pallets containing

very small amount of sample. Scanning electron microscope (SEM) was taken by LEO instrument (model- VP 1450, Germany) in order to identify the surface morphology of ZnO-NP-AC (AS). X-ray diffraction (XRD) pattern was collected with an automated Philips X'Pert X-ray diffractometer.

2.3. Preparation of ZnO-NP-AC (AS)
2.3.1. Carbonization of AS and modification with acid

In first step, almond shells were used as a precursor for preparation of carbon. They were firstly washed with distilled water to remove

impurities and dried overnight in an oven at 80 °C. Then, they were ground and loaded into crucible. They were placed in furnace and heated to 300°C for 2 h to produce carbon. The resultant product was cooled to room temperature and sieved into a uniform size (80-100mesh). In order to modify the surface of carbon, they were soaked in mixture of HNO_3: HCl (1:1) with mass ratio 2:1 (weight of carbon: weight of mixture of HNO_3 and HCl) while stirred on the magnetic stirrer for 24h. The resultant surface modified carbon (AC (AS)) washed with distilled water for several times to separate excess acids.

2.3.2. Synthesis of ZnO-NP

ZnO-NP was synthesized by hydrothermal method based on the reaction of zinc acetate (Zn (CH3COO)) with NaOH at autoclave reactor placed in furnace. The mixture was heated by specific temperature programming until 180°C for

36-48h. Then, it was rapidly cooled in water and ice bath. Obtained ZnO-NP washed with deionized water and was placed in an oven at 65°C for 7h.

2.3.3. Mixing the modified carbon with ZnO-NP

Synthesized ZnO-NP was physically mixed with the carbon modified by acid in weight ratio of 1:4 (weight of NP: weight of modified carbon). Final product (ZnO-NP-AC (AS)) was used as an efficient adsorbent for removal of dyes.

2.4. Preparation of dye solutions

The stock solutions of BB41and BR46 dyes were prepared in 1.0 g/L concentration. The test solutions containing desired concentrations of BB41 and BR46 were prepared by diluting 1.0 g/L of stock solutions of BB41 and BR46 and mixing them in the test medium. Before adding ZnO-NP-

AC (AS) as adsorbent, the pH of test solution was adjusted to optimum value with concentrated HNO_3 and NaOH solutions.

2.5. Measurements of dyes adsorption

According to the experiments designed though CCD method, 50mL of desired concentrations of dyes in binary solution were prepared and then, were added into a 250 mL erlenmeyer flask containing spesific amounts of adsorbent. The experiments were performed at room temperature and desired sonication time in ultrasonic bath. At the end of the adsorption experiments, the sample was immediately centrifuged and then the supernatant containing residual dyes was spectrophotometrically analyzed by measuring the absorbance of the solution. The removal percentage of each dye (R%) was calculated by:

$$(R\%) = \frac{C_0 - C_t}{C_0} \tag{1}$$

Where C_0 (mg/L) and C_t (mg/L) are the dye concentration at initial and after time t, respectively.

The adsorbed amount of each dye at equilibrium, qe (mg/g), was calculated by:

$$q_e = \frac{V(C_0 - C_e)}{M} \tag{2}$$

Where C_0 is the initial dye concentration (mg/L), C_e is the residual dye concentration at equilibrium state (mg/L), V is the volume of the solution (L), and M is the weight of the adsorbent (g).The dyes

concentration was obtained by calibration curves at the wavelength determined by derivative and normal spectroscopy (411.5, 607 nm for BR46 and BB41 that obtained by first and zero order derivative spectra respectively). Origin Pro 9.1softwarewas used for derivation of zero order spectra.

2.6. Experimental design

In the present work, the central composite design (CCD) was chosen for modeling and optimization of the ultrasonic assisted simultaneous removal of BB41and BR46 in binary solution by using ZnO-NP-AC (AS) as an adsorbent. The Software used for design of experiment (DOE) was Design Expert 8. A five-level CCD with four factor (sonication time (X_1),

adsorbent dosage (X_2), BB41concentration (X_3), BR46 concentration (X_4)) was used to investigate the effects of factors. The experimental range and levels of independent variables are shown in Table 2.The condition of 31 experiments designed by CCD in addition to dyes removal percentages (response (R %)) are given in Table 3.

3. Results and discussion

3.1. Characterization of adsorbent

As shown in Fig. 1, In order to investigate the surface functional groups of acid modified carbon (AC (AS)), FT-IR spectrum were studied in the range of $4000 - 400\ cm^{-1}$.The broad band in the range of 2400-3200 cm^{-1}was assigned to stretching vibration of the hydroxyl functional groups. In addition, the bands at about 1710 and 1230 was probably corresponded to the C=O and C-O stretching vibration.

The X-ray patterns of ZnO nanoparticles and its references are shown in Fig. 2. The main X-ray peaks of ZnO-NPs was appeared at 2θ=30.54, 33.92, 35.74, 46.85, 55.69, 62.19, 65.70, 67.33, 68.63 which was in good agreement with the X-ray diffractogram of its references. The mean size of ZnO-NPs is calculated by:

$$d = \frac{k\lambda}{D\cos\theta} \tag{3}$$

Where k is a dimensionless shape factor, with a value close to unity (0.9) but varies with the actual shape of the crystallite, λ is the X-ray wavelength, θ is the Bragg angle in degrees, D is the line broadening at half the maximum intensity (FWHM) which denoted its quantity as 2θ; d is the mean size of the ordered (crystalline) nanoparticles in angstrom. Therefore the mean size of ZnO-NPs was found to be 45nm.

The surface morphological features of modified carbon by acid and ZnO nanoparticles loaded on modified carbon (ZnO-NP-AC(AS)) were represented in Fig. 3 (a,b). The pore formation in the carbon structure is mainly attributed to the addition of mixture of HNO_3 and HCl which causes the carbon to swell and it opens the surface structure. Fig. 3(b) indicates the morphology of ZnO nanoparticles loaded on modified carbon are spherical and their size are found in range of 20-100 nm which placed in the pores of modified carbon with acid.

Table 2. The experimental range and levels of independent variables in CCD.

Independent variables	Ranges and levels				
	-α	-1	0	+1	+ α
(X_1) Adsorbent dosage (g)	0.01	0.02	0.03	0.04	0.05
(X_2) Sonication time (min)	8	12	16	20	24
(X_3) BR41 concentration (mg/L)	10	13.75	17.50	21.25	25
(X_4) BR46 concentration (mg/L)	5	8.75	12.50	16.25	20

Table 3. CCD for four independent variables with the observed responses.

runs	X_1 (g)	X_2 (min)	X_3 (mg/L)	X_4 (mg/L)	R_1 (%)	R_2 (%)
1	0.04	12	13.75	8.75	83.01	76.75
2	0.03	16	17.50	12.50	78.30	71.51
3	0.04	20	21.25	16.25	88.51	78.91
4	0.02	20	13.75	8.75	83.02	75.49
5	0.04	12	21.25	16.25	77.56	68.20
6	0.03	16	17.50	12.50	77.91	69.58
7	0.03	8	17.50	12.50	69.74	66.23
8	0.04	20	13.75	16.25	95.47	83.95
9	0.02	20	21.25	8.75	75.65	69.75
10	0.02	12	13.75	16.25	73.38	61.23
11	0.02	20	13.75	16.25	77.09	69.28
12	0.02	20	21.25	16.25	72.18	64.47
13	0.05	16	17.50	12.50	91.95	82.25
14	0.03	16	17.50	12.50	76.26	70.32
15	0.03	24	17.50	12.50	92.35	84.39
16	0.02	12	21.25	16.25	71.05	60.76
17	0.04	12	13.75	16.25	80.26	72.08
18	0.01	16	17.50	12.50	64.82	58.52
19	0.04	20	13.75	8.75	95.39	89.45
20	0.03	16	17.5	12.50	77.72	72.70
21	0.03	16	17.5	5.00	78.80	80.93
22	0.03	16	17.5	12.50	78.87	71.95
23	0.03	16	17.5	12.50	79.10	73.18
24	0.03	16	25.00	12.50	72.33	67.27
25	0.03	16	17.50	21.25	79.58	62.38
26	0.03	16	17.50	12.50	78.88	71.44
27	0.02	12	13.75	8.75	74.48	67.39
28	0.02	12	21.25	8.75	69.59	65.37
29	0.03	16	10.00	12.50	82.63	73.51
30	0.04	12	21.25	8.75	76.69	75.43
31	0.04	20	21.25	8.75	91.16	86.72
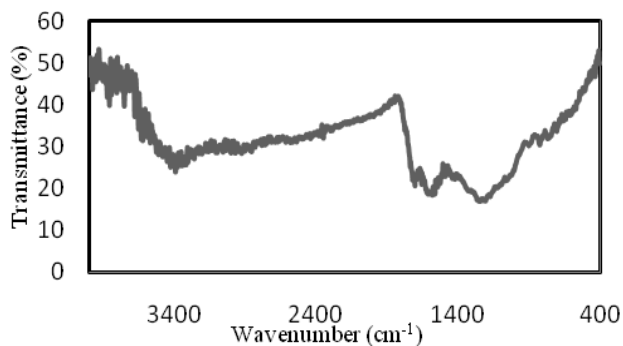
Fig.1. FT-IR spectra of AC (AS).

3.2. Derivative and normal spectroscopy

Zero order absorption spectra of BR46 and BR41 in single and binary solutions are shown in Fig.4. Unlike the BR41 dye analysis, which its concentration is easily obtained at 607nm (maximum absorbance in single solution of BR41) spectra, the BR46 dye concentrations cannot in be determined at 530 nm in their mixture. For resolving this problem, derivative spectrophotometry method is suillustrated in Fig. 5.
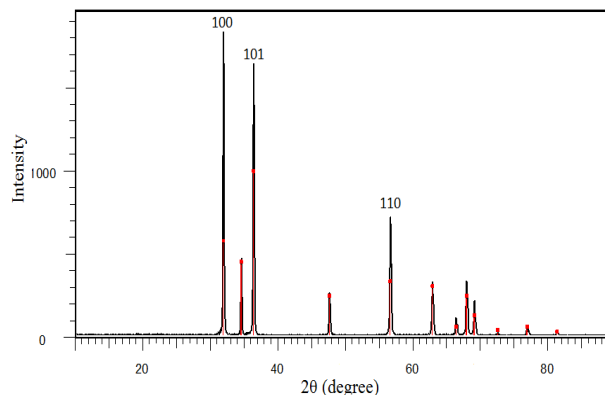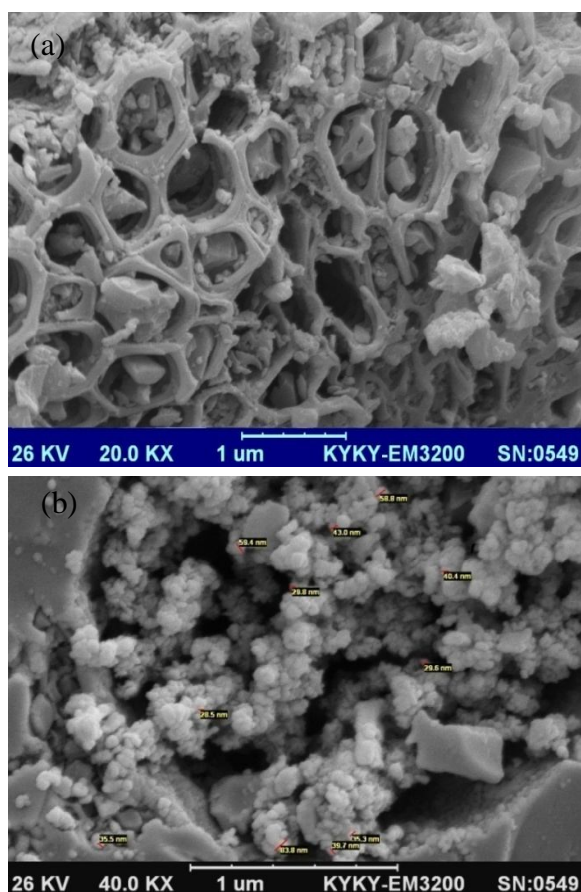
Fig. 2. XRD pattern of ZnO-NP.

Fig. 2. SEM image of (a) AC (AS) and (b) ZnO-NP-AC (AS).

Tthe first order derivative spectra of BB41 is zero at 411.5 nm in single solution that can be used for the quantitative determination of BR46 in binary solution. In order to investigate the accuracy of wavelength obtained through first order

derivative, the percentage of recoveries and relative errors for the binary solutions with different concentrations of each dye are studied (that given in Table 4) by the following equation

$$(\%)Recovery = \frac{C_m}{C_t} \times 100 \qquad (4)$$

$$(\%)Error = \frac{C_m - C_t}{C_t} \qquad (5)$$

Where C_t, C_m are the theoretical and measured concentrations, respectively. The measured concentrations were calculated by three types of calibration curves obtained from the binary solutions with different concentrations of each dye. The error percentage less than 5 (or recovery percentage in range of 95-105) indicates the first order derivative spectrophotometric and normal spectrophotometric methods possess sufficient accuracy for the simultaneous analysis of BR46 and BB41, respectively.
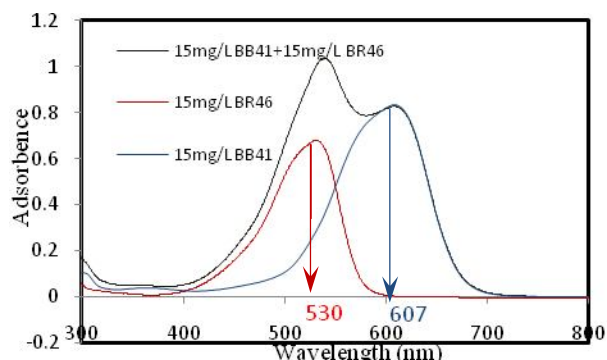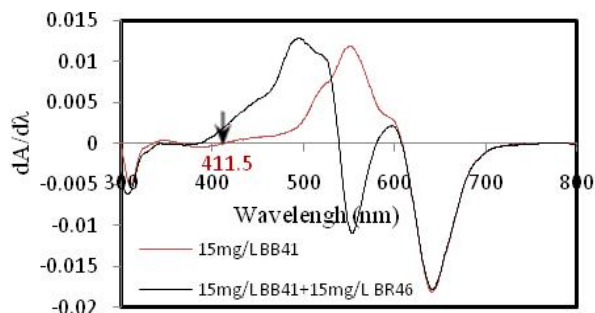

Fig. 4. Zero order absorption spectra of BR46 and BR41 in single and binary solution.

3.3. The effect of the initial pH on the adsorption of BB41 and BR46

The value of pH not only changes the surface charge of adsorbent, but also, influences on the ionization amount of adsorbates. Therefore, the small changes of pH can significantly affect on the removal percentage. In order to investigate the effect of pH, seven experiments were performed in

the pH range of 2-8 at specified values of other parameters which represented in Fig.6.

Fig. 5. First order absorption spectra of BR46 and BR41 in single and binary solution.

As the pH increases, the removal percentage of two dyes enhance until pH 6, after that, the dyes removal slowly decreases. In fact, the adsorption mechanism is mainly followed by ion exchange via releasing exchangeable proton in the interlayer and basal plane surfaces. Hydronium ions are adsorbed more easily than cationic dyes due to higher

mobility and small size. So that, decreasing of the amount of H^+ causes to reduce of competition of H^+ and cationic dyes in adsorption and increases the dyes removal efficiency.
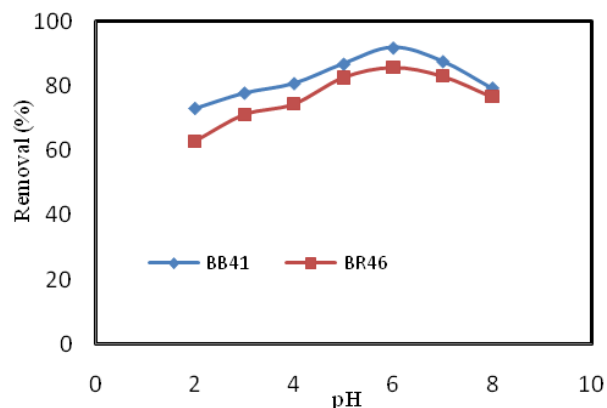
Fig. 6. The effect of pH on the removal percentage of Basic Red 46 and Basic Blue 41 by ZnO–NP–AC (conditions: 19 min of sonication time, 0.03 g of adsorbent dosage, 14 mg/L of BR46 and 9 mg/L of BB 41 dyes in 50 mL of binary solution at room temperature).

Table 4. Recovery and error percentage for BB41 and BR46 at 607,411.5 nm in binary solution by zero and first order derivative spectra, respectively.

Theoretical concentrations (mg/L)		Measurement concentrations (m		Recovery (%)		Error (%)	
C_{BB41}	C_{BR46}	C_{BB41}	C_{BR46}	C_{BB41}	C_{BR46}	C_{BB41}	C_{BR46}
5	5	4.84	5.20	96.80	104.00	-3.20	+4.00
10	5	10.25	5.13	102.50	102.60	+2.50	+2.60
15	5	15.21	4.87	101.40	97.40	+1.40	-2.60
20	5	19.43	4.85	97.15	97.00	-2.85	-3.00
25	5	25.57	4.79	102.28	95.80	+2.28	-4.20
30	5	30.07	5.37	100.23	107.40	+0.23	+7.40
5	5	4.75	5.20	95.00	104.00	-5.00	+4.00
5	10	4.76	10	95.20	100.00	-4.80	0.00
5	15	4.86	15.16	97.20	101.06	-2.80	+1.06
5	20	5.17	19.77	103.40	98.85	+3.40	-1.15
5	25	4.76	25.38	95.20	101.52	-4.80	+1.52
5	30	5.13	30.5	102.60	101.66	+2.60	+1.66
5	5	4.77	4.75	95.40	95.00	-4.60	-5.00
10	10	10.33	10.40	103.30	104.00	+3.30	+4.00
15	15	15.26	15.30	101.73	102.00	+1.73	+2.00
20	20	20.53	20.80	102.65	104.00	+2.65	+4.00
25	25	25.75	24.41	103.00	97.64	+3.00	-2.36
30	30	30.92	29.45	103.06	98.16	+3.06	-1.83

3.4. Central composite design

As shown in Table1,the independent variables (sonication time (X_1), adsorbent dosage (X_2), BB BR41concentration (X_3), BR46 concentration (X_4)) are given the coded form (-α, -1, 0, +1, +α). The value of α, represents the number of axial point(star points) and depends to the number of factors (k).The value of α is evaluated by:

$$\alpha = 2^{k/4} = 2 \qquad (6)$$

Table 5. ANOVA in CCD for BB41dye.

Source of variation	Sum of squares	Degree of freedom	Mean square	F-value	P-value
X_1	886.59	1	886.59	322.39	<0.0001
X_2	576.93	1	576.93	209.79	<0.0001
X_3	151.55	1	151.55	55.10	<0.0001
X_4	8.49	1	8.49	3.08	0.0984
$X_1 X_2$	70.43	1	70.43	25.61	0.0001
$X_1 X_3$	0.032	1	0.032	0.011	0.9178
$X_1 X_4$	1.32	1	1.32	0.48	0.4984
$X_2 X_3$	3.27	1	3.27	1.18	0.2935
$X_2 X_4$	6.83	1	6.83	2.48	0.1349
$X_3 X_4$	2.18	1	2.18	0.79	0.3873
X_1^2	2.22	1	2.22	0.80	0.3844
X_2^2	25.36	1	25.36	9.22	0.0079
X_3^2	0.081	1	0.081	0.029	0.8669
X_4^2	7.34	1	7.34	2.66	0.1224
Lack of fit	38.27	10	3.827	3.95	0.0532
Pure error	5.79	6	0.965		
Total SS	1780.7	30			

Table 6. ANOVA in CCD for BR46 dye.

Source of variation	Sum of squares	Degree of freedom	Mean square	F-value	P-value
X_1	878.58	1	878.58	472.35	<0.0001
X_2	478.20	1	478.20	257.09	<0.0001
X_3	61.73	1	61.73	33.18	<0.0001
X_4	301.64	1	301.64	162.17	<0.0001
$X_1 X_2$	31.16	1	31.16	16.75	0.0008
$X_1 X_3$	0.0003	1	0.0003	0.0001	0.9921
$X_1 X_4$	0.54	1	0.54	0.29	0.5976
$X_2 X_3$	7.06	1	7.06	3.79	0.0693
$X_2 X_4$	0.28	1	0.28	0.15	0.7036
$X_3 X_4$	0.36	1	0.36	0.19	0.6687
X_1^2	0.79	1	0.79	0.42	0.5261
X_2^2	32.22	1	32.22	17.32	0.0007
X_3^2	0.78	1	0.78	0.41	0.5310
X_4^2	1.12	1	1.12	0.60	0.4499
Lack of fit	20.27	10	2.027	1.27	0.4006
Pure error	9.54	6	1.59		

| Total SS | 1828.18 | 30 |

The CCD consists of a 2k factorial runs with 2k axial runs and n_0 centre runs. So, the total number of experiments (N) is calculated by:

$$N = 2^k + 2k + n_0 = 16 + 8 + 7 = 31 \qquad (7)$$

In order to obtain true relationship between the dependent variable and the set of independent variables, the following second-order polynomial equation is proposed:

$$Y = \beta_0 + \sum_{i=1}^{4}\beta_i X_i + \sum_{i=1}^{4}\sum_{j=1}^{4}\beta_{ij} X_i X_j + \sum_{i=1}^{4}\beta_{ii} X_i^2$$

$$(8)$$

Where Y is the predicted response (removal percentage), Xi and Xj are independent variables (sonication time, adsorbent dosage, BB41 and BR46 dye concentrations), β_0 is the constant model,

β_i, β_{ii} and β_{ij} are coefficients for the linear,

quadratic and interaction effects, respectively BB46dye:

$$Y = 71.53 + 6.05X_1 + 4.46X_2 - 1.60X_3 - 3.53X_4 + 1.40X_1X_2 + 1.10X_2^2$$

(9)

BB41 dye:

$$Y = 78.15 + 6.08X_1 + 4.90X_2 - 2.51X_3 - 0.78X_4 + 1.40X_1X_2 + 0.93X_2^2 \qquad (10)$$

The amounts of R-squared and Adj R-squared for BB41dye were found to be 0.9750 and 0.9531 respectively that were close to each other. This means that, the difference between experimental and the predicted responses is negligible where

shown in Fig.7. For BB46 dye, the values of R-squared was almost similar to Adj R–squared (R-squared=0.9812, Adj R –squared=0.9647). Fig.8 represents the correlation between experimental and predicted data.

3.5. Response surface methodology

To investigate the interactive effect of four factors on the removal of each dye, the response surface methodology (RSM) was used. Fig.8 (a,b) represent the interaction of adsorbent dosage and sonication time in removal of BB41 and BB46dyes, respectively.The curvatures of these plots indicate the interaction between the variables. In other words, as sonication time and adsorbent dosage increase, dyes removal percentage improves. This means that, the mass transfer of dye molecules enhances on the surface of adsorbent and adsorption process quickly reaches equilibrium state. Also, by increasing the adsorbent dosage, further surface area of adsorbent is available for dyes molecules leads to enhance the dyes removal percentage.

3.6. Optimization of CCD using the desirability function (DF)

In numerical optimization, desirability is a function that ranges from zero, outside of the limits, to one at the goal. So, it was selected desired goal for each factor and for response obtaining the maximum dyes removal efficiency with high desirability function (close to one) for each dye. This goals could be changed maximize, minimize, target, in range, none (only for responses).Therefore, the optimum condition for each factor were found to be 0.03 g of adsorbent dosage, 19 min of sonication time, dye

concentration of 19 mg/L for BB41 and 9 mg/L for BR46 resulted in maximum dyes removal (85% and 91%for BR46 and BB41, respectively).
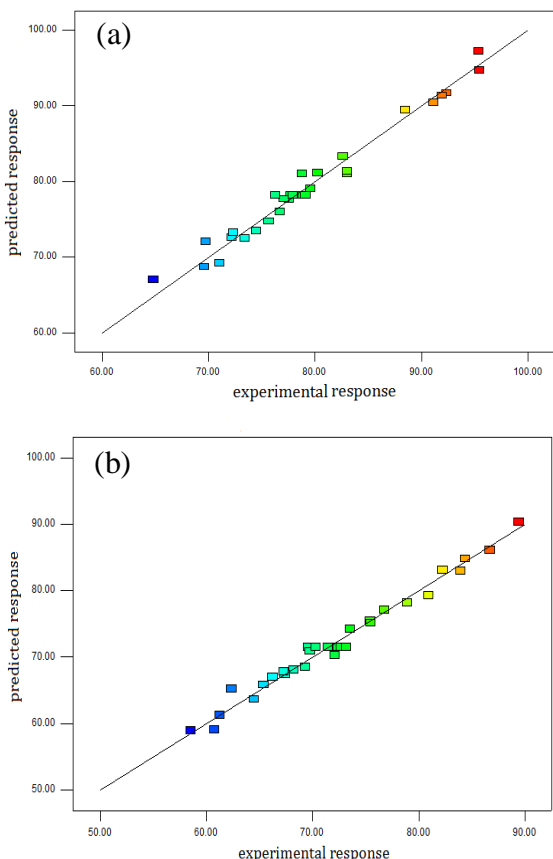

Fig. 7. The experimental data versus the predicted data of normalized removal of (a) BB41 and (b) BB46 dyes.

3.7. Adsorption equilibrium study
Several isotherm models including Langmuir, Freundlich, Tempkin can be applied for evaluating the equilibrium properties of adsorption
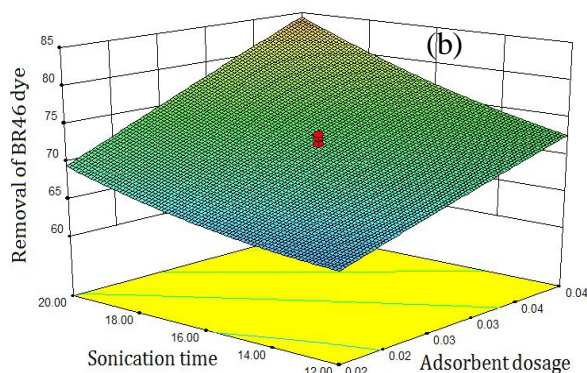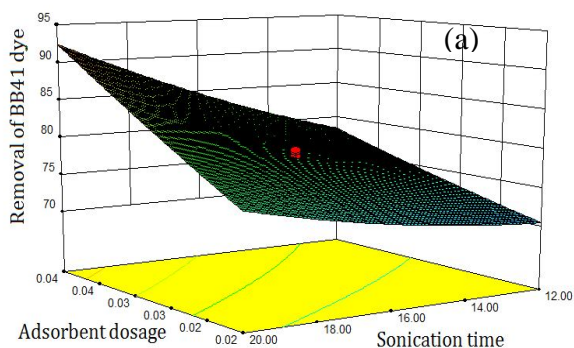

Fig. 8. 3D surface plot of Removal of (a) BB41 dye and (b) BR46 dye; versus adsorption dosage and sonication time

residual dye concentration and the amount of absorbed dye at equilibrium state in the constant temperature. The widely used Langmuir isotherm has been found successful application in many real sorption processes. Unlike Freundlich isotherm, adsorption of molecules in Langmuir isotherm model occurs as a monolayer on the equivalence sites of adsorbent without any adsorbate-adsorbate interactions. A linear form of Langmuir isotherm can be expressed by:

$$\frac{C_e}{q_e} = \frac{1}{K_L q_{max}} + \frac{C_e}{q_{max}} \tag{11}$$

Where C_0 (mg/L), q_e (mg/g) are the dye concentration and the amount of absorbed dye at equilibrium state respectively. q_{max} (the maximum amount of absorbed dye) and K_L (Langmuir constant) are calculated from slope and intercept of linear plot of $\frac{C_e}{q_e}$ versus C_e, respectively. The

dimensionless parameter named separation factor (RL) is introduced in Langmuir's model to indicate the favorability of the adsorption and is determined by:

$$R_L = \frac{1}{1+K_L C_0} \tag{12}$$

In order to accept the Langmuir isotherm model, the value of R_L should be found between one and zero $(0 < R_L < 1)$. Freundlich isotherm is often used for equilibrium description in adsorption systems with heterogeneous surface energy that its linear form can be given by:

$$Log q_e = Log K_f + \frac{1}{n} Log C_e \tag{13}$$

The slope and intercept of the linear plot of $Log q_e$ versus $Log C_e$ indicate $\frac{1}{n}$ (heterogeneity index) and K_F (Freundlich constant), respectively. The dimensionless parameter of $\frac{1}{n}$ varies from 0 to 1, with 1 being homogeneous and values approaching zero being increasingly heterogeneous.

In binary systems, due to competition between components for adsorption sites, extended Freundlich and the P-Factor models is often applied for equilibrium description. In P-Factor model, the amount of absorbed dye for each component of binary solution in equilibrium state ($q_{e,e}$) is calculated by:

$$q_{e,i,binary} = \frac{K_{L,i}^0 C_{e,i,binary\,solution}}{P_i [1 + K_{L,i}^0 C_{e,i,binary\,solution}]} \tag{14}$$

P_i (p-factor) is the dimensionless parameter that is expressed by:

$$P_i = \frac{(K_{L,i}/R_{L,i})_{single\,solution}}{(K_{L,i}/R_{L,i})_{Binary\,solution}} \tag{15}$$

Where $K_{L,i}/R_{L,i}$ is adsorbent monolayer capacity for component i that is calculated in single and

binary systems. Related equations of extended Freundlich have been explained in literatures[14].The constant parameters and correlation coefficients obtained from the P-Factor and the extended Freundlich isotherm models are summarized in Table 7. Because of high correlation coefficient (R^2), P-Factor model showed the reasonable agreement to adsorption equilibrium data.

$$\tag{13}$$

Table 7. Isotherm parameters for adsorption of basic dyes onto the ZnO-NP-AC(AS).

Isotherm model	BB41 dye	BR46 dye
P-Factor		
R^2	0.999	0.999
q_{max}	0.6035	0.442
The amount of P-Factor	1.013	2.798
extended Freundlich		
R^2	0.993	0.955
n	0.031	12.98
K_F	13.99	26.81

3.8. Adsorption kinetic study

In order to examine the rate of the adsorption process, a suitable kinetic model such as pseudo-first-order, pseudo-second-order, Elovich and intraparticle diffusion is needed to analyze the mechanism of chemical reaction. The linear form of pseudo-first-order equation is expressed by:
Where k_1 (rate constant, min-1), q_e (the amount of adsorbed dye at equilibrium state, mg/g) can be obtained from the slop and intercept of the linear plot of $\log(q_e - q_t)$ versus t, respectively. As shown in Table 8, the value of correlation coefficient, R^2, for each dye in this model was low. Therefore pseudo-first-order equation cannot predict the rate and mechanism of the adsorption process. Following linear equation illustrates pseudo-second-order model.

$$\frac{t}{q_t} = \frac{1}{k_2 q_e^2} + \frac{t}{q_e} \qquad (17)$$

Table 8. Kinetic parameters for adsorption of basic dyes onto the ZnO-NP-AC(AS).

Kinetic model	BB41 dye	BR46 dye
pseudo-first-order		
R^2	0.944	0.918
k_1	0.1082	0.168
q_e(calc)	17.70	8.810
q_e(exp)	25.95	12.75
pseudo-second-order		
R^2	0.982	9.993
k_2	0.00568	0.0222
q_e(calc)	29.25	14.70
q_e(exp)	25.95	12.75
Elovich		
R^2	0.921	0.925
β	0.156	0.356
α	15.573	16.164
intraparticle diffusion		
R^2	0.967	0.92
K_{diff}	4.324	1.852
C	6.180	5.302

$$log(q_e - q_t) = \frac{-k_1 t}{2.303} + log q_e \qquad (16)$$

In this model, the slop and intercept of linear plot of $\frac{t}{q_t}$ versus t can indicate k_1 (rate constant, g/mg.min) and q_e (mg/g), respectively. The value of R^2 for each dye not only was found to be close to one, but also the difference between calculated and experimental q_e was low and negligible (Table 8).

So, pseudo-second-order model is a suitable kinetic model for explaining the rate of the adsorption process. Elovich and intraparticle diffusion models are other kinetic models that their linear equations are given by Eqs.18, 19 respectively.

$$q_t = \frac{1}{\beta} ln(\alpha\beta) + \frac{1}{\beta} ln(t) \qquad (18)$$

$$q_t = K_{dif} t^{1/2} + C \qquad (19)$$

The values of R^2 in addition to the amount of constant models are presented in Table 8.

As shown in Table 8, the values of R^2 in Elovich and intraparticle diffusion models were found to be lower than pseudo-second-order model that indicates they aren't efficient models in description of adsorption kinetic.

4. Conclusion

In this research, acid modification in addition to the application of ZnO nanoparticles for carbon derived from agricultural waste such as almond shell caused to produce an efficient adsorbent for removal of dyes from binary solution. In order to analyze dyes in binary solution, derivative spectrophotometric method was used. Application of ultrasonic bath improved the simultaneous removal of BB41 and BR46 in binary solution. This means that; in comparison of the magnetic stirrer and in the same condition, the time of removal was decreased from 40 min to 19 min. the optimum condition for the maximum simultaneous removal of dyes in binary solution was obtained by CCD combined RSM and DF. Finally; the equilibrium and kinetic studies revealed that the experimental data were in good agreement to the P-Factor and pseudo-second-order models, respectively.

References

[1] B.H. Hameed, F.B.M. Daud, Chem. Eng. J. 139 (2008) 48-55.

[2] A.C. Ueda, L.H. de Oliveira, N. Hioka, M.n. Aznar, J. Chem. Eng. Data. 56 (2011) 652-657.

[3] M. Celebi, M.A. Kaya, M. Altikatoglu, H. Yildirim, J. Sci. Techol., 3 (2013) 39-45.

[4] N.M. Mahmoodi, M. Arami, H. Bahrami, S. Khorramfar, Desalination. 264 (2010) 134-142.

[5] R. Jian-min, W. Si-wei, J. Wei, World Academy of Sci. Eng. Technol, 41 (2010) 05-23.

[6] E. Yagmur, J Porous Mater. 19 (2012) 995-1002.

[7] C. Shendkar, , R. Torane, K. Mundhe, S. Lavate, N. Deshpande,J. Pharm. Pharm. Sci. 5 (2013) 527-529.

[8] R. Hoseinzadeh Hesas, W.M.A. Wan Daud, J.N. Sahu, A. Arami-Niya, J. Anal. Appl. Pyrolysis. 100 (2013) 1-11.

[9] P. Pragya1, S. Sripal, Y. Maheshkumar, Res. J. Chem. Sci. 3 (2013) 12-15.

[10] S.X. Liu, X. Chen, X.Y. Chen, Z.F. Liu, H.L. Wang, J. Hazard. Mater. 141 (2007) 315-319.

 [11] P. K. Chayande, S .P. Singh, M. K. N. Yenkie,Chem. Sci. Trans. 2 (2013) 835-840.

[12] M. Ghaedi, A. Ansari, R. Sahraei, Spectrochim. Acta, Part A. 114 (2013) 687-694.

[13] M. Ghaedi, S.J.Hossaini, S. Ramezani, E-J. Chem. 9 (2012) 63-74.

[14] M. Ghaedi, S. Hajati, B. Barazesh, F. Karimi, G. Ghezelbash,J. Ind. Eng. Chem. 19 (2013) 227-233.

[15] M. Turabik, J. Hazard. Mater. 158 (2008) 52-64.

[16] F. Rasouli, S. Aber, D. Salari, A.R. Khataee, Appl. Clay Sci. 87 (2014) 228-234.

[17] S.C. Papita Das Saha, Subhabrata Das, Arch. Environ.Sci. 6 (2012) 57-61.

[18] M. Demirel, B. Kayan, Int. J. Ind. Chem, 3 (2012) 1-10.

[19] M. Roosta, M. Ghaedi, N. Shokri, A. Daneshfar, R. Sahraei, A. Asghari, Spectrochim. Acta, Part A. 118 (2014) 55-65.

[20] M. Roosta, M. Ghaedi, A. Daneshfar, R. Sahraei, Spectrochim. Acta, Part A. 122 (2014) 223-231.